Detailed molecular dynamics simulation of the self-diffusion of *n*-alkane and *cis*-1,4 polyisoprene oligomer melts

V. A. Harmandaris and M. Doxastakis
Institute of Chemical Engineering and High Temperature Chemical Processes, ICE/HT-FORTH, GR 26500 Patras, Greece, and Department of Chemical Engineering, University of Patras, 26500 Patras, Greece

V. G. Mavrantzas[a)]
Institute of Chemical Engineering and High Temperature Chemical Processes, ICE/HT-FORTH, GR 26500 Patras, Greece

D. N. Theodorou
Institute of Chemical Engineering and High Temperature Chemical Processes, ICE/HT-FORTH, GR 26500 Patras, Greece, and Department of Chemical Engineering, University of Patras, 26500 Patras, Greece

(Received 7 August 2001; accepted 18 September 2001)

Results are presented for the self-diffusion properties of monodisperse *n*-alkanes and *cis*-1,4 polyisoprene (PI) oligomer melts, as obtained through detailed atomistic molecular dynamics (MD) simulations. The simulations have been conducted in the *NVT* statistical ensemble on model systems thoroughly pre-equilibrated through an efficient Monte Carlo (MC) algorithm. Results for the self-diffusion coefficient D as a function of molecular weight M support a scaling law of the form $D \sim M^b$, with b strongly depending on temperature T, for both the *n*-alkanes and the *cis*-1,4 PI melts. The simulation results have been fitted to an expression for D involving elements of Rouse dynamics and Cohen–Turnbull–Bueche chain-end (excess free volume) effects, proposed recently by von Meerwall *et al.* [J. Chem. Phys. **108**, 4299 (1998)]. Using a geometric analysis involving tessellation of space in Delaunay tetrahedra developed by Greenfield and Theodorou [Macromolecules **26**, 5461 (1993)], we have also calculated the excess chain-end free volume of the alkane and *cis*-1,4 PI melts. Calculated self-diffusivities and apparent activation energies for the two different polymers as a function of their molecular weight M are in excellent agreement with the experimental measurements of von Meerwall *et al.* (1998). © *2002 American Institute of Physics.* [DOI: 10.1063/1.1416872]

I. INTRODUCTION

An accurate knowledge of the transport properties of polymeric liquids is extremely important in technological applications, since these properties govern their processability in the molten state. Efforts to predict these properties through either theoretical arguments or detailed computer simulation studies have attracted considerable interest in the literature. In addition to predicting the diffusion properties of pure polymer melts, the mutual diffusion properties of such polymers in binary mixtures with smaller molecules are also of great importance. Experimental efforts with state-of-the-art techniques to measure the self- and binary diffusion properties of such systems have also been reported.[1,2]

From the theoretical point of view, polymer dynamics seems to be governed to a large extent by the molecular weight of the constituent chains: For melts with molecular weight M less than the molecular weight for the formation of entanglements M_e, the Rouse model predicts that the self-diffusion coefficient D should scale with M as M^{-1}. For melts with M greater than M_e, the pure reptation theory predicts that $D \sim M^{-2}$. Phenomena such as contour length fluctuations (CLF) and constraint release (CR) typically accelerate the escape of the chain from the confining topological constraints, and this causes an increase in D and a decrease in the zero-shear rate viscosity η_0. Thus, a recently proposed theory that incorporates CLF and CR phenomena predicts a stronger exponent for D, between -2.2 and -2.3.[3] These values agree quite well with recent experimental results for concentrated polymer solutions and melts, which suggest an exponent between -2.2 and -2.4 for a variety of polymer systems in the entangled regime.[4]

Experimentally, the diffusion properties of polymeric systems in the liquid state are measured with pulsed-gradient spin–echo NMR methods.[5,6] Systematic measurements with systems such as *n*-paraffins and polyisoprene (PI) melts in the past and recent years suggest a strong dependence of the diffusion coefficient D on both molecular mass M and temperature T. For unentangled chains, in particular, D follows, at least approximately, a scaling law of the form

$$D(M,T) = AM^b, \tag{1}$$

where b is a strong function of temperature T. For chains that are neither too short nor too long (entangled), b equals -1, as predicted from the Rouse theory. On the other hand,

[a)]Author to whom correspondence should be addressed. Electronic mail: vlasis@iceht.forth.gr

smaller chains (in the sub-Rouse regime) are found to exhibit a stronger dependence of diffusion properties on chain length, with b significantly lower than -1.

The above scaling laws have been tested very recently through very long, detailed atomistic MD simulations of model PE melt systems, with mean molecular length ranging from C_{78} up to C_{250}. In all these simulations, the equations of motion were integrated with the rRESPA (reversible REference System Propagator Algorithm) multiple time step (MTS) algorithm, first proposed by Tuckerman *et al.*,[7] which allowed very long simulations, up to 300 ns, at $T=450\,\mathrm{K}$ and $P=1$ atm.[8]

According to these simulation findings, a plot of the self-diffusion coefficient D as a function of the molecular length for lengths up to C_{250} exhibits three distinct regions: (a) A small-molecular weight, alkane-like region (for molecular lengths $N<60$) where D follows a power-law dependence $D\sim M^{-b}$ with an exponent b greater than 1. As we will see in detail in this paper, system dynamics in this regime is dominated by chain-end effects, which can be described through a free-volume theory.[9] (b) An intermediate, Rouse-type regime (for molecular lengths ranging from $N=60-70$ up to $N=156$) where the exponent b is practically 1, and (c) A long chain-length, reptation-like regime (for molecular lengths $156<N<250$) where chain diffusivity exhibits a dramatic slowdown, the exponent b being close to 2.5. As mentioned in the previous paragraph, the latter agrees well with the predictions of the modified reptation theory incorporating contour length fluctuations (CLF) and constraint release (CR) mechanisms.

Of interest here is the dependence of the self-diffusion coefficient D on M for the shorter chain lengths in the sub-Rouse regime, and how it is affected by the temperature T. The steeper exponent which is observed in this regime is usually attributed to an additional host effect. This can be comprehensively described through the free-volume theory,[10–12] particularly in connection with the concept of the excess free volume of chain ends relative to that of interior segments along the chain (chain-end free volume). The fraction of free volume provided by chain ends is assumed to be inversely proportional to M so that its effects increasingly enhance D at low M. The resulting expression for the diffusion coefficient is then a combination of Rouse diffusion and chain-end free-volume host effects. To test this hypothesis, very recently, in a series of papers, von Meerwall *et al.*[13,14] documented the diffusion of strictly monodisperse *n*-alkanes and *cis*-1,4 PI melts in a range of temperatures T. They confirmed the power-law form of D and found very good agreement for the diffusion both in *cis*-1,4 PI and in *n*-alkane melts with the combined theory. Von Meerwall *et al.*[13] also derived the apparent thermal activation energies of the self-diffusion coefficient as a function of M.

In the present work, new results will be presented about the dependence of the self-diffusion coefficient on molecular length and temperature from detailed atomistic MD simulations with model, strictly monodisperse *n*-alkane, and *cis*-1,4 PI oligomer melts.

This work is a part of a systematic approach for the prediction of the volumetric, structural, and transport properties of polyolefins and polydienes either in their pure molten state or in mixtures with a smaller molecular weight penetrant molecule. The direct prediction of the solubility of *n*-alkanes and oligomers in long-molecular weight PE melts has been addressed through the design of two novel, very efficient MC moves, fusion and scission.[15] With these two new moves, results were obtained for the sorption isotherms of C_5, C_{10}, and C_{20} in molten linear PE and their dependence on the average chain length of the polymer matrix, and compared extensively to available experimental data and to calculations based on the Flory–Huggins theory and the SAFT equation of state (EoS). In another work, the prediction of the diffusion coefficient of small alkanes in a polymer matrix is addressed with MD simulations.[16] At the same time, a hierarchical approach has been developed for predicting the diffusive behavior of small-molecular weight substances through a structurally disordered polymer by means of kinetic MC simulations.[17] Work is also in progress related to the prediction of the structural and dynamic properties of *cis*-1,4 PI melts through a parallel-tempering end-bridging MC method.[18]

The present paper addresses the dependence of the self-diffusion of melts of *n*-alkanes and *cis*-1,4 PI oligomers on molecular weight and temperature. Results will be reported for: (a) the density ρ and (b) the self-diffusion coefficient D, of *n*-alkane liquids (with molecular length ranging from C_{16} to C_{60}) and *cis*-1,4 PI liquids (with molecular length between C_{20} and C_{60}) as a function of the molecular weight M of the melt and the temperature T. In all cases, the simulation results are compared against the recent experimental data of von Meerwall *et al.*[13] and the predictions of the combined Rouse–free-volume theory. To elucidate the role of the excess chain-end free volume, we have explicitly calculated the free volume of chain ends relative to that of atoms deeper along the chain, following the methodology proposed by Greenfield and Theodorou.[19] Thus, results will also be presented for the excess free volume of chain ends over middle chain atoms and its dependence on temperature.

The paper is organized as follows. Section II presents the molecular model and the simulation strategy followed to study the self-diffusion of monodisperse oligomers in atomistic detail. Section III reviews the basic elements of a free-volume theory based on the concept of the chain-end free-volume host effect, as reported by Bueche[9] and von Meerwall *et al.*[13] Results from the atomistic MC and MD simulations for the density, free volume, and self-diffusion coefficient of the *n*-alkane and *cis*-1,4 PI liquids and their dependence on molecular weight and temperature are presented in Sec. IV and compared directly against the experimentally measured data. The major conclusions of the work are summarized in Sec. V.

II. MOLECULAR MODEL, SIMULATION STRATEGY, AND SYSTEMS STUDIED

A. *n*-alkane and polyethylene melts

For the representation of the *n*-alkane and PE melts, a united-atom description is used in the present work, with each methylene or methyl group considered as a single

Lennard-Jones (LJ) interaction site. Site–site intra- and intermolecular interactions are defined according to a model proposed by Mondello *et al.*[20] Nonbonded interactions are described by a LJ potential of the form

$$V_{\mathrm{LJ}}(\mathbf{r}) = 4\varepsilon\left[\left(\frac{\sigma}{\mathbf{r}}\right)^{12} - \left(\frac{\sigma}{\mathbf{r}}\right)^{6}\right], \tag{2}$$

with $\varepsilon = 0.093$ kcal/mol for CH_2, $\varepsilon = 0.227$ kcal/mol for CH_3, and $\sigma = 4.01$ Å for both CH_2 and CH_3. V_{LJ} describes all intermolecular site–site interactions as well as intramolecular interactions between sites separated by more than three bonds. The interaction parameters between a CH_2 and a CH_3 site are determined by the Lorentz–Berthelot rules

$$\varepsilon_{\mathrm{CH_2-CH_3}} = \sqrt{\varepsilon_{\mathrm{CH_2}}\varepsilon_{\mathrm{CH_3}}}, \quad \sigma_{\mathrm{CH_2-CH_3}} = \frac{\sigma_{\mathrm{CH_3}} + \sigma_{\mathrm{CH_2}}}{2}. \tag{3}$$

A potential cutoff distance of 9.062 Å is used. Attractive tail contributions were dealt with through direct integration.[21]

A bond-bending potential of the form

$$V_{\mathrm{bending}}(\theta) = \tfrac{1}{2}K_{\theta}(\theta - \theta_0)^2, \tag{4}$$

is also used for every skeletal bond angle with $K_{\theta} = 124.18$ kcal mol^{-1} rad^{-2} and $\theta_0 = 114°$. Associated with each dihedral angle ϕ is a torsional potential of the form

$$V_{\mathrm{torsional}}(\phi) = \sum_{i=0}^{3} c_i(\cos\phi)^i, \tag{5}$$

with $c_0 = 1.736$, $c_1 = 4.500$, $c_2 = 0.764$, and $c_3 = -7.000$, all in kcal/mol. Furthermore, adjacent methyl and methylene groups are maintained at a fixed distance $l = 1.54$ Å using the SHAKE method.[22,23]

With the above model, the following *n*-alkane systems have been simulated:

(i) A 50-chain C_{16} melt, at temperatures $T = 323$, 343, 383, 403, and 443 K.
(ii) A 35-chain C_{26} melt, at temperatures $T = 323$, 343, 383, 403, and 443 K.
(iii) A 35-chain C_{36} melt, at temperatures $T = 343$, 383, 403, and 443 K.
(iv) A 30-chain C_{44} melt, at temperatures $T = 343$, 383, 403, and 443 K.
(v) A 16-chain C_{60} melt, at temperatures $T = 383$, 403, and 443 K.

Key to the dynamic simulations reported in this work is a multiple time step (MTS) algorithm, which has allowed us to track the evolution of the systems studied for very long times, up to 300 ns.[8] The method employed is the reversible REference System Propagator Algorithm (rRESPA), first proposed by Tuckerman *et al.*[7] and subsequently used in the simulation of *n*-alkanes[24] and hydrocarbon blends.[25] This is a time-reversible algorithm based on the separation of the Liouville operator into two different operators. The first includes fast modes which are integrated with a small time step dt. The second describes the slow motions of the molecules, which are integrated with a larger time step D$t = i$dt, where i is an integer (usually between 1 and 10). Consequently, the number of computationally expensive evaluations of the relatively slowly varying LJ forces, which is usually the most time-consuming part in the MD simulations, is significantly reduced for a given overall simulation time. To control the temperature, an implementation of the Nosé–Hoover algorithm in the rRESPA scheme, the XI-RESPA algorithm, was used.[7,26,27] Using rRESPA, we have been able to speed up the calculations involved in a typical NVT MD method by 2–5 times over conventional MD algorithms. In all simulations reported in the present study, the smaller time step dt was taken equal to 1 fs and the larger time step Dt equal to 5dt, i.e., 5 fs, the overall simulation time ranging from 10 to 60 ns, depending on the length of the *n*-alkane and the temperature.

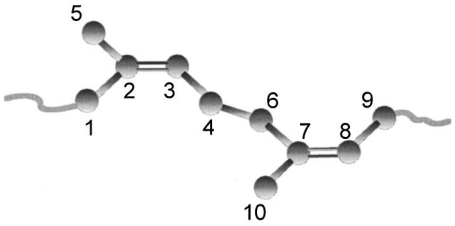

FIG. 1. Model view of a two-monomer segment of a *cis*-1,4 PI chain.

B. *cis*-1,4 polyisoprene melts

The model used in our *cis*-1,4 PI simulations employs a united-atom description (see Fig. 1) and is based on a polybutadiene model proposed by Smith and Paul[28] and Smith *et al.*[29] For intermolecular interactions as well as intramolecular interactions between sites separated by more than three bonds, a LJ potential was used with the cutoff distance set at $R_{\mathrm{cutoff}} = 10$ Å. A similar model has been employed in our recent parallel-tempering end-bridging MC simulation study of the same polymer.[18] Although bond lengths were kept constant as in the recent MC work, bond angles were allowed to vary subjected to harmonic potentials in order to represent more accurately the local dynamics of the polymer chain. The detailed form and the parameters of the potentials used in the simulations of the *cis*-1,4 PI melts are reported in Tables Ia and b.

The MD simulation of the *cis*-1,4 PI melts was performed with the YASP 3.0[30] molecular dynamics program. Constant-temperature simulations were executed using Berendsen's thermostat, together with a leapfrog scheme to integrate the equations of motion. Rigid bond constraints were implemented following the SHAKE algorithm. A timestep of 1 fs was used in all time integrations.

Four *cis*-1,4 PI systems were studied in this paper, all consisting of the same total number of united atoms (equal to 840):

(i) a 42-chain C_{20} melt (degree of polymerization 4);
(ii) a 28-chain C_{30} melt (degree of polymerization 6);
(iii) a 21-chain C_{40} melt (degree of polymerization 8); and
(iv) a 14-chain C_{60} melt (degree of polymerization 12).

The simulation temperatures were: 353, 373, 393, and 413 K. The simulation time varied between 20 and 40 ns, depending on the molecular length of the polymer studied.

TABLE I. (a) Lennard-Jones parameters for the pair interactions used in our *cis*-1,4 PI model. (b) Force field parameters for *cis*-1,4 PI (see Fig. 1 for notation).

(a)	i	j	ε_{ij} (kcal/mole)	$r_{\min,ij}$ (Å)
	$C^{=}$	$C^{=}$	0.100 0	3.8
	$C^{=}$	$CH^{=}$	0.100 0	3.8
	$C^{=}$	CH_2	0.101 5	4.257
	$C^{=}$	CH_3	0.150 5	4.257
	$CH^{=}$	$CH^{=}$	0.100 0	3.8
	$CH^{=}$	CH_2	0.101 5	4.257
	$CH^{=}$	CH_3	0.150 5	4.257
	CH_2	CH_2	0.093 6	4.5
	CH_2	CH_3	0.145 6	4.5
	CH_3	CH_3	0.226 4	4.5
	CH_3 (4)	CH_2 (10)	0.007 28	4.5

(b)	Bending potential $V_\theta = 1/2 k_\theta (\theta - \theta_0)^2$ (Ref. 28)			k_θ (kJ mol^{-1} rad^{-2})	Bond angle θ_0 (deg)
	CH_2 (1)	C (2)	CH (3)	374.0	125.9
	C (2)	CH (3)	CH_2 (4)	374.0	125.9
	CH (3)	CH_2 (4)	CH_2 (6)	481.16	111.65
	CH_3 (5)	C (2)	CH (3)	374.0	125.9
	CH_2 (4)	CH_2 (6)	C (7)	481.16	111.65

Harmonic dihedral potential $V_h = 1/2 k_\varphi (\varphi - \varphi_0)^2$				k_φ (kJ mol^{-1} rad^{-2})	Dihedral angle φ_0 (deg)
CH_2 (1)	C (2)	CH (3)	CH_2 (4)	160	0
CH_3 (5)	C (2)	CH (3)	CH_2 (4)	160	180

Torsional potential $V_\varphi = 1/2 \Sigma k_n (1 - \cos n\varphi)$ (Ref. 29)	k_n (n=1,...,6) (kJ/mol)					
4–6–7–8	3.598	−0.167	4.853	0.669	1.590	−0.502
2–3–4–6	3.598	−0.167	4.853	0.669	1.590	−0.502
3–4–6–7	−4.142	−2.594	−16.903	−0.293	−1.046	−0.795

For both the *n*-alkane and the *cis*-1,4 PI oligomer melts, the simulation protocol involved three stages: First, an initial configuration was generated by applying the amorphous cell method of Theodorou and Suter,[31] followed by a potential energy minimization. With this minimum-energy configuration, detailed atomistic MC simulations were executed in the *NPT* statistical ensemble to equilibrate the system fully at the desired temperature.[32] The density values reported in this paper were obtained through these MC simulations without involving the connectivity-altering end-bridging move,[18,32] in order to maintain the simulated systems strictly as monodisperse. The relaxed configurations at the end of the MC runs were then used as starting configurations in the subsequent MD runs in the *NVT* statistical ensemble to obtain the dynamic properties of the two polymer systems.

III. FREE-VOLUME THEORY

According to the free-volume theory, the diffusive properties of short molecules in the sub-Rouse regime are controlled by the availability of free volume in the system. More specifically, the total volume in the liquid is divided into two components: the occupied volume and the free volume. Molecular transport is presumed to rely on the continuous redistribution of free-volume elements within the liquid. The free-volume theory was originally proposed by Cohen and Turnbull[1,10] and was further developed by many others.[11–13] Bueche proposed that the higher mobility of chains in short-chain melts is mainly due to the significant effect of the extra free volume around chain ends.[9]

More recently, the theory was revised by von Meerwall *et al.* to take into account the simultaneous Rouse and free-volume effects.[13] According to this approach, the self-diffusion is predominantly Rouse in character, but corrections need to be made to account for the significant effect of the excess free volume in these systems due to chain ends. The following general expression for the self-diffusion coefficient in short-chain, monodisperse polymer melts is reported:[13]

$$D(M,T) = A \exp(-E_a/RT) M^{-1} \exp[-B_d/f(T,M)], \tag{6}$$

where the prefactor A is a constant characterizing the particular polymer but otherwise independent of chain length and/or temperature. One can distinguish three terms in Eq. (6). The first exponential term describes thermal activation effects, with E_a being the thermodynamic activation energy required for a segment to perform jumps between accessible

neighboring sites. This, in fact, is a measure of the energy required for the chain to break free from its neighbors before moving into a contiguous free-volume void. The second term (M^{-1}) recognizes the Rouse dependence of the diffusivity on the diffusant molecular length or mass. And, the last term represents the contribution to the self-diffusion coefficient due to the excess free volume of chain ends. B_d is a volume overlap parameter, while f plays the role of a fractional free volume, which is highly dependent on T and on M at low molecular weights.

The fractional free volume is described by the following equation:

$$f(T,M)=f(T,\infty)+2V_e(T)\rho(T,M)/M, \tag{7}$$

that is, by the sum of two terms: The first represents the segmental hole free volume and depends only on temperature. The second is a chain-end contribution to free volume: V_e is the chain-end free volume existing in addition to the regular contribution of the last monomer in units of cm^3 per (mol of chain ends). Expression (7) for the fractional free volume can be solved for the mass density of the melt through

$$\rho(T,M)=[1/\rho(T,\infty)+2V_e(T)/M]^{-1}. \tag{8}$$

That is, the inverse mass density (specific volume) has the form of a hyperbolic function of molecular weight. Clearly

$$f(T,M)-f(T,\infty)=1-\frac{\rho(T,M)}{\rho(T,\infty)}. \tag{9}$$

A more detailed description of the free-volume theory and the chain-end free volume host effects is given elsewhere.[9,13]

IV. RESULTS

Results will be presented about the density and self-diffusion coefficient of linear monodisperse alkanes of length ranging from C_{16} to C_{60} and of *cis*-1,4 PI melts of 20 to 60 carbon atoms, as a function of temperature and molecular weight. The results will be analyzed in terms of the concept of the Bueche–von Meerwall free-volume theory that combines Rouse diffusion with chain-end free volume effects. In all cases, the results are directly compared to the experimental data for the corresponding systems published by von Meerwall *et al.*[13,14]

A. Density of liquid *n*-alkanes and PI oligomers

Figure 2 shows results for the density ρ of the liquid *n*-alkanes as a function of molecular weight, at $T=443\,K$ (filled circles). Also shown in the figure (open circles) are the experimentally measured density values.[13] It is seen that the density ρ increases quickly with M, particularly at low M. The rate with which ρ increases with m is constantly decreasing, and above C_{60}, ρ seems to approach a constant value, which for the *n*-alkanes studied here is a unique function of the temperature T. The figure also shows that, overall, the agreement with the experimentally measured densities is satisfactory. For all *n*-alkanes studied, the maximum deviation between the predicted and the measured values is less than about 2%, which agrees with the results of our previous

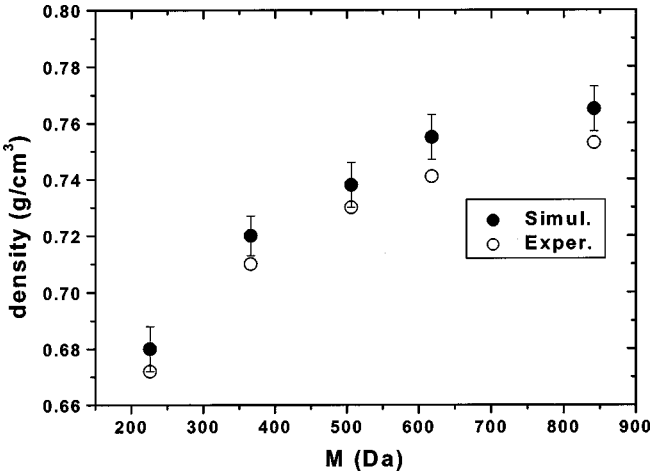

FIG. 2. Simulation predictions for the density ρ of liquid *n*-alkanes (filled circles) and experimentally measured values (open circles), as a function of their molecular weight M, at $T=443\,K$.

study with significantly longer PE melts. The same level of agreement holds true also for the other temperatures studied.

Figure 3 shows in detail the model predictions for ρ as a function of the length of the *n*-alkane, for all temperatures investigated. Each ρ versus M curve can be separately fitted to Eq. (8) by adjusting the two parameters $\rho(T,\infty)$ and $V_e(T)$. The first denotes the value of the density at infinite M, and the second the excess free volume of chain ends; both parameters are functions of temperature only. All fits (solid lines in Fig. 3) are seen to be particularly satisfactory, which allows us to extract the temperature dependence of $\rho(T,\infty)$ and $V_e(T)$; this is demonstrated in Fig. 4. Both $1/\rho(T,\infty)$ and $V_e(T)$ are seen to vary exactly linearly with T, in agreement with the Cohen–Turnbull proposition

$$1/\rho(T,\infty)=a+bT=1.1+0.000\,95T(^\circ C),$$

$$V_e(T)=c+dT=15.85+0.063T(^\circ C). \tag{10}$$

The corresponding experimental values are[13]

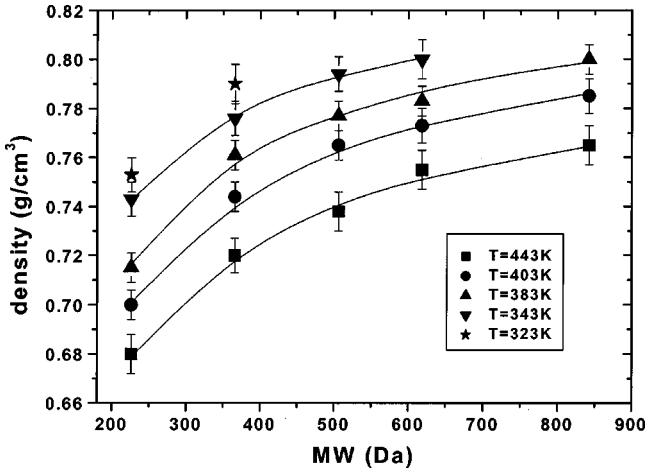

FIG. 3. Simulation predictions for the density ρ of the liquid *n*-alkanes as a function of their molecular weight M, at different temperatures.

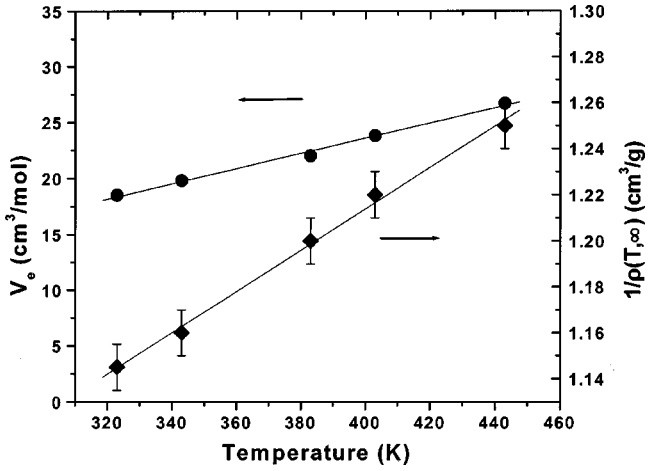

FIG. 4. Temperature dependence of the parameters V_e and $1/\rho(T,M)$ for the *n*-alkane melts. The results have been obtained by fitting the simulation predictions for the density ρ to Eq. (8).

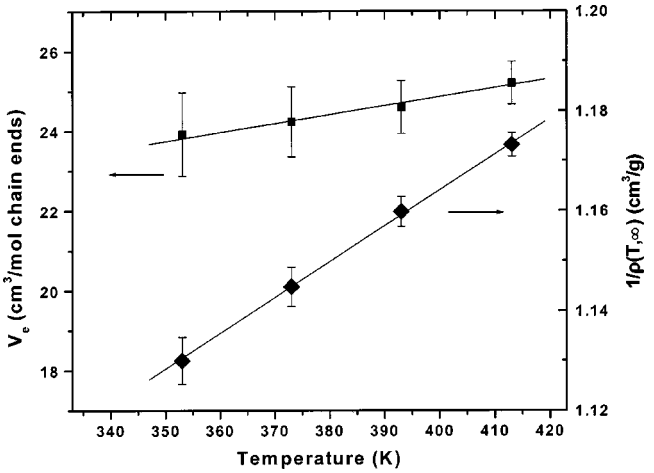

FIG. 6. Temperature dependence of the parameters V_e and of the quantity $1/\rho(T,M)$ for the *cis*-1,4 PI melts. The results have been obtained by fitting the simulation predictions for the density ρ to Eq. (8).

$$1/\rho(T,\infty)=a+bT=1.142+0.000\,76T(^\circ\mathrm{C})$$
$$V_e(T)=c+dT=13.93+0.06T(^\circ\mathrm{C}), \tag{11}$$

with the temperature expressed in °C. The good qualitative and quantitative agreement with the experimental data is expected given the consistency of the simulation predictions for the density of these systems with the corresponding measured values.

For the *cis*-1,4 PI oligomers, no experimental density values are available in the literature for the systems studied here, to the best of our knowledge. However, in recent MC simulations with polydisperse PI melts,[18] we have compared $\rho(T,\infty)$ from simulations with long PI chains to experimentally available data[33] and found good agreement (within 2%) for the entire temperature range between 328 and 513 K. The simulation data were also compared against analytical expressions for $\rho(T,\infty)$ proposed in the literature. The densities of the monodisperse *cis*-1,4 PI melts simulated in this work are very close to those of the corresponding polydisperse melts of the same mean molecular weight.

The densities of the monodisperse *cis*-1,4 PI melts, as derived from the present MC simulations, as a function of the molecular weight M of the melt are plotted in Fig. 5. In the same figure, a point has been included at each temperature denoting the density of a polydisperse C_{80} ($M=1090$ g/mol) melt that was equilibrated using the parallel tempering end-bridging MC method,[18] which allows vigorous sampling of the configuration space of the system, resulting in fast equilibration even at low temperatures. The agreement with the MC simulation predictions based on the current monodisperse samples for $M<900$ g/mol is quite satisfactory.

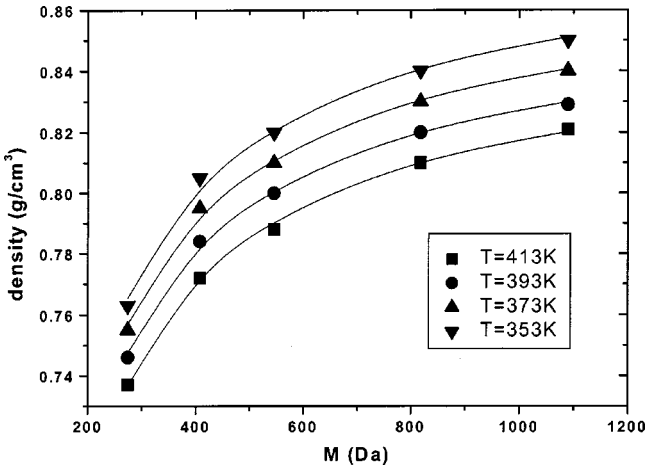

FIG. 5. Molecular weight dependence of the density of the *cis*-1,4 PI melts.

Fitting the density data to Eq. (8) gives estimates of the chain-end free volume V_e also for the *cis*-1,4 PI melts. These are plotted in Fig. 6, together with the values of $\rho(T,\infty)$. The free-volume values are similar to those of the PE melts. Their temperature dependence cannot be assessed safely, but, clearly, the free volume as estimated from the density data is much larger than the value of 13.7 or 6.9 cm^3/(mol chain ends) reported in Ref. 14, derived from self-diffusion measurements.

The parameter V_e, the free volume of chain ends, plays a particular role in the theory of Bueche. According to his definition, "free volumes as discussed here refer only to packets of free volume that are too large to reach nearly instantaneous equilibrium at temperatures which are below T_g."[9] Thus, to get more insight into V_e, we carried out a direct calculation of the free volume in the systems investigated here, following the geometric analysis proposed by Greenfield and Theodorou.[19] The method conducts first a tessellation of space into Delaunay tetrahedra, considering the center of every LJ unit as a point in space. A Delaunay tetrahedron corresponds to four neighboring atoms surrounding a small "hole" in the bulk polymer. The size of the atoms is then increased to their corresponding van der Waals radii and a calculation of the empty space inside each Delaunay tetrahedron is carried out. The unoccupied volume corresponding to each atom is calculated by summing the unoccupied volumes of all tetrahedra in which the reference atom participates.

The free volume around each atom in the *n*-alkane sys-

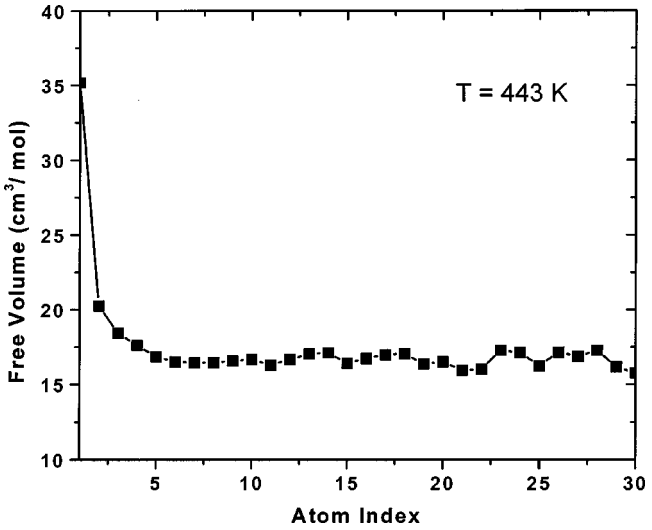

FIG. 7. Values of the geometrically calculated free volume V^g around a chain atom as a function of the position or rank number of the atom along the chain backbone. The results have been obtained by the method proposed by Greenfield and Theodorou (Ref. 19) involving tessellation of the model systems in Delaunay tetrahedra.

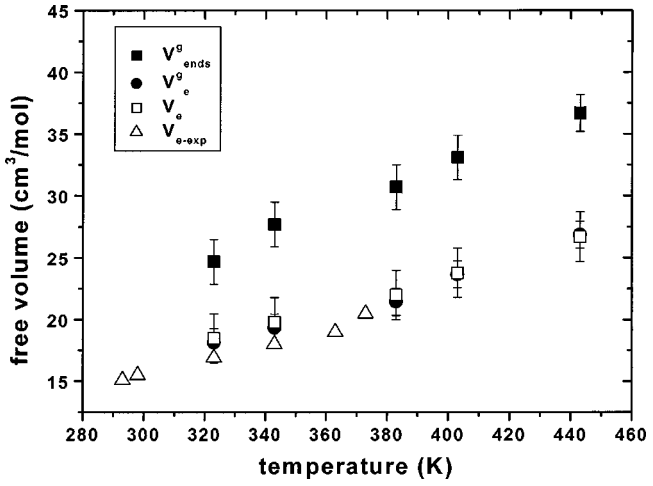

FIG. 8. Values of the free volume V^g_{ends} calculated geometrically by the method of Greenfield and Theodorou (Ref. 19) around chain ends (filled squares) and values of the geometrically calculated chain-end free volume V^g_e (filled circles). Also shown in the figure are results for the chain-end free volume V_e calculated by fitting the densities to Eq. (8) (open squares) and experimentally available data for V_e (open triangles) (Ref. 13).

tems studied in the present work, as a function of its position along the chain, as calculated by applying the Greenfield–Theodorou approach for the C_{60} melt at $T=443$ K, is shown in Fig. 7. Clearly, the distribution of free volume along the chain should be symmetric around the chain midpoint. It is also seen that the free volume around chain ends is significantly higher than the free volume around inner atoms along the chain; this is a result of the nonconnectivity of chain ends. Figure 7 shows that, typically, nonuniformities in the distribution of free volume along the chain persist over only a region of 4 to 5 atoms from the two chain ends. Beyond this region, the distribution becomes uniform.

The unoccupied volume around chain ends, V^g_{ends} (the superscript g being used to denote free volumes calculated by the geometric analysis of Greenfield and Theodorou) varies significantly with temperature. This variation is shown in Fig. 8 be the filled squares. The values reported in the figure have been obtained after a thorough calculation over hundreds of different configurations accumulated during both the *NPT* MC and the *NVT* MD simulations and averaged over all *n*-alkane melts simulated. Also shown in the figure by the triangles are the values of V_e derived from the experimental densities. It is seen that the two values follow the same behavior with T. However, the calculated values are systematically higher than those extracted experimentally. This should have been expected, given that V_e should refer not to the entire unoccupied volume around chain ends but to packets of free volume greater than a ''critical'' value. If it is assumed that this critical value is the unoccupied free volume around the interior atoms in the chain V^g_{inner}, then one can define a geometric chain-end (excess) free volume, V^g_e, through the relation

$$V^g_e=\sum_{i=1}^{k}(V^g_i-V^g_{\text{inner}}), \tag{12}$$

where k is the number of atoms for which V^g is higher than V^g_{inner} (typically $k=4-5$ as shown in Fig. 7). How this changes with T and how it compares to the values of free volume extracted indirectly from the experimental densities is shown in Fig. 8 by the filled circles. Remarkably, the values of chain-end free volume V^g_e calculated geometrically through Eq. (12) are practically the same as those obtained from the fittings to the predicted densities and are also very close to those extracted experimentally.

The definition of the chain-end free volume through Eq. (12) is consistent with the usual interpretation of V_e [see Eq. (7)] as the free volume around chain ends in excess of that generated near any segment in the chain. In general, in diffusion studies of a small penetrant molecule through a polymer matrix, one distinguishes between two types of free volume: the unoccupied free volume and the accessible free volume. The unoccupied free volume is the total free volume in the polymer. The accessible free volume is that part of the total (or unoccupied) free volume through which the penetrant molecule can diffuse, and is calculated based on the probe radius of the molecule. In the present study, the accessible free volume is calculated based on a probe radius equal to the size of adjacent molecular segments, which also controls intermolecular distance. Thus, Eq. (12) gives in essence the accessible free volume for the diffusion of a chain segment around the ends of the chain, in addition to that generated near any other segment along the chain.

The free volume per mole of atoms in the *cis*-1,4 PI chains varies significantly with the atom-ranking position along the chain, due to the different chemical architecture of this polymer as compared to PE. Figure 9 presents the geometric free volume as extracted for the five different atom types in a PI monomer as a function of the monomer position in the chain, according to the method described above, for a C_{60} *cis*-1,4 PI liquid (12 monomers per chain) at $T=413$ K and $P=1$ atm. It is seen that atom types 1, 3, and 4 (see Fig. 1 for notation) have similar free volumes when placed far

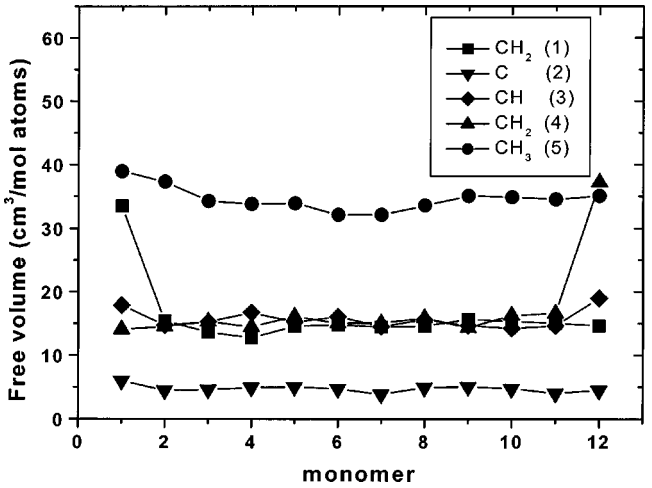

FIG. 9. Free volume per mole of atoms of a C_{60} (12 monomers) *cis*-1,4 PI chain at $T=413$ K and $P=1$ atm. The different numbers denote the different types of atoms in a PI monomer (see Fig. 1).

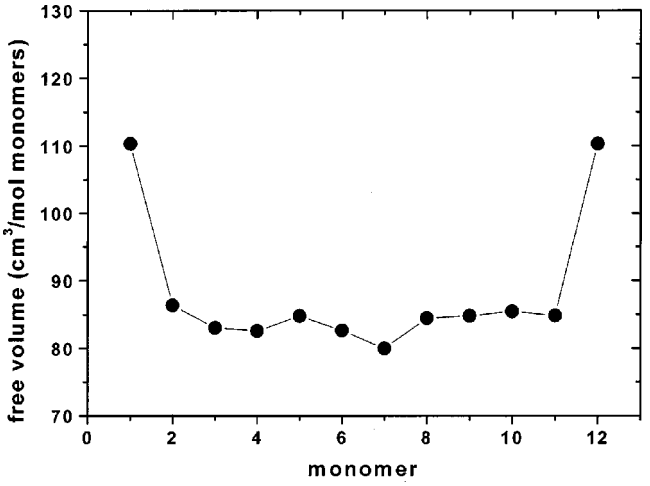

FIG. 10. Free volume per mole of monomers of a C_{60} (12 monomers) *cis*-1,4 PI chain at $T=413$ K and $P=1$ atm.

from the chain ends. On the other hand, atom types 2 and 5 are characterized by significantly different free volumes. Atoms of type 2 are ''surrounded'' by the other atoms of the same monomer which are directly connected to them (atom types 1,3,5), and this considerably limits the amount of free volume around them. The opposite holds for the methyl substituent (CH_3): This, being a side atom to the main chain, experiences a much larger (by a factor of 2 to 3) free volume than any other atom in the PI chain. This happens because methyl groups of one chain like to lie opposite to the methyl groups of neighboring chains and, therefore, find themselves apart from segments of backbone atoms along the same chain.[18]

Another feature that deserves special attention is that *cis*-1,4 PI is a nonsymmetric molecule. This means that the start of a chain (atoms of type 1 or 5; see Fig. 1) is different from the end of the chain (atoms of type 4). As a result, atoms of type 1 in Fig. 9 are characterized by a higher free volume when examined at the start of the chain (first atom from the start) than at the end of the chain (fourth atom from the end of the chain). The same holds for all atom types in a PI monomer. In fact, a very careful examination of the figure shows that an atom of type 4 at the end of the chain (first atom from the end) has slightly more free volume than an atom of type 1 at the start of the chain (first atom from the start). This last result is clearly due to the presence of the methyl group (atom of type 5). Therefore, in order to extract the free volume of a chain end one has to consistently define a chain end for a *cis*-1,4 PI chain. The most convenient choice is to define a chain end as a whole monomer at the start or at the end of a chain. Adding up the free volumes of all atoms in a particular monomer gives the points drawn in Fig. 10. The figure clearly suggests that by considering atoms in groups of 5 (i.e., entire monomers), the free volume experienced by monomers is different only for those being at the ends of the chain. Figure 11 compares the free volume of chain ends (defined as end monomers) and of monomers belonging to the interior of the chain. Their difference, at a particular temperature, defines the geometrically calculated chain-end free volume V_e^g exactly as in the case of the *n*-alkane melts. Results for V_e^g for the *cis*-1,4 PI oligomers studied are in very good agreement with the corresponding values of the free volume obtained through the densities of these systems (see Fig. 5). The mean value obtained from this analysis is seen to differ significantly from the value of 6.9 cm^3/mol (chain ends) reported in Ref. 14 through fittings of the self-diffusion measurements and follows the corresponding values for the *n*-alkane melts.

B. Self-diffusion coefficient

The self-diffusion coefficients D of the melts simulated with the MD method are determined with the help of the Einstein relation. D is calculated from the slope of the mean-square displacement of the chain centers of mass, $\langle (R_{cm}(t)-R_{cm}(0))^2 \rangle$, through

$$D=\lim_{t\to\infty}\frac{\langle (R_{cm}(t)-R_{cm}(0))^2\rangle}{6t}. \tag{13}$$

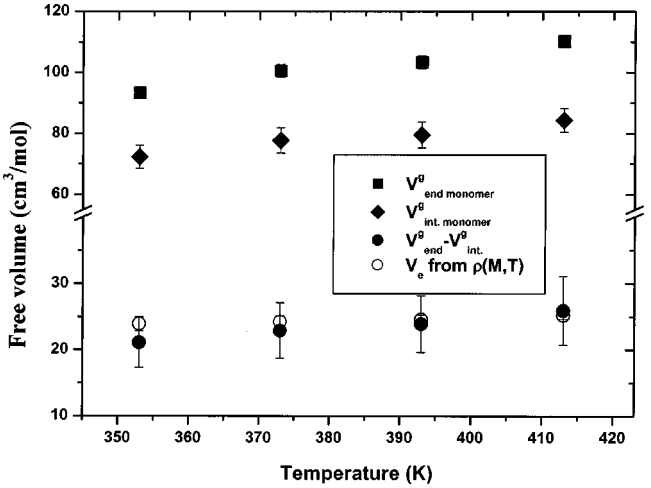

FIG. 11. Free volume of the *cis*-1,4 PI monomers at the end of the chain (filled rectangles) and in its interior (filled diamonds). Their difference, defining the geometrically chain-end free volume V_e^g, is also shown in the figure by the filled circles and is compared to the values obtained from density fittings (open circles).

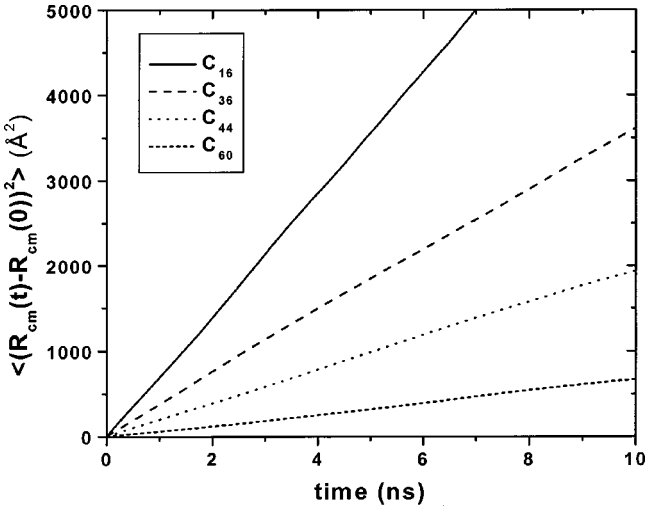

FIG. 12. Typical plots of the mean-square displacement of the chain centers of mass as a function of time for the C_{16}, C_{36}, C_{44}, and C_{60} *n*-alkane systems, obtained from the present *NVT* MD simulations with the rRESPA multiple time-step algorithm ($T=443$ K).

TABLE II. (a) Simulation results for the value of the exponent *b* quantifying the dependence of the self-diffusion coefficient *D* on molecular weight *M*, obtained by fitting the MD simulation predictions to the power law of Eq. (1) for the *n*-alkane melts. Experimentally measured *b* values are also shown. (b) Simulation results for the value of the exponent *b* quantifying the dependence of the self-diffusion coefficient *D* on molecular weight *M*, obtained by fitting the MD simulation predictions to the power law of Eq. (1) for the *cis*-1,4 PI oligomer melts.

		$b(T)$	
(a)	T (K)	Simulation predictions	Experimental values
	343	−2.4	−2.35
	383	−2.26	−2.18
	403	−2.1	−2.04
	443	−1.9	−1.88

		$b(T)$
(b)	T (K)	Simulation predictions
	353	−2.6
	373	−2.3
	393	−2.3
	413	−2.0

Typical plots of the mean-square displacement of the chain centers of mass as a function of time *t*, for most of the *n*-alkanes studied (C_{16}, C_{36}, C_{44}, and C_{60} at $T=443$ K), are shown in Fig. 12. It is seen that, in the long-time regime, all curves reach an asymptotic, linear behavior, characteristic of Fickian diffusion, the slope of which can be used to determine *D* according to Eq. (13). Results for *D* for all melts simulated as a function of the molecular weight and the system temperature are shown in Fig. 13. Also shown in Fig. 13 are the experimentally measured *D* values from the NMR experiments[13] at $T=403$ K. The agreement is extremely good for the majority of the alkanes studied.

Also interesting is that the best fits of the diffusivities to the power-law expression of Eq. (1) are almost perfect (solid lines in Fig. 13), with the exponent *b* quantifying the dependence of *D* on the molecular weight *M* of the alkanes varying smoothly in the temperature range studied ($b=-2.4$ at 343 K, while $b=-1.9$ at 443 K), as shown in Table II(a).

From Arrhenius plots of the $\log D$-versus-$1/T$ curves, we can extract the thermal activation energies of the melts studied and compare them directly to the values measured experimentally. In particular, we can calculate the apparent activation energies E_a^{app} for self-diffusion in an *n*-alkane melt through the equation:

$$E_a^{\mathrm{app}} = -\frac{R}{0.434}\frac{\partial(\log D)}{\partial(1/T)}. \tag{14}$$

Results for the *M* dependence of E_a^{app} are shown in Fig. 14, together with the experimental data. It is seen that E_a^{app}

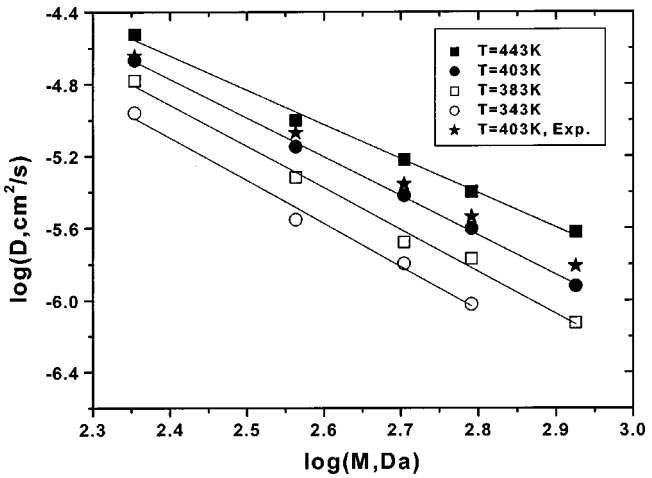

FIG. 13. Simulation predictions for the self-diffusion coefficient *D* of the *n*-alkane liquids, as a function of their molecular weight at different temperatures. A detailed comparison of the scaling exponent b with the experimental data of von Meerwall *et al.* (Ref. 13) is given in Table II(a).

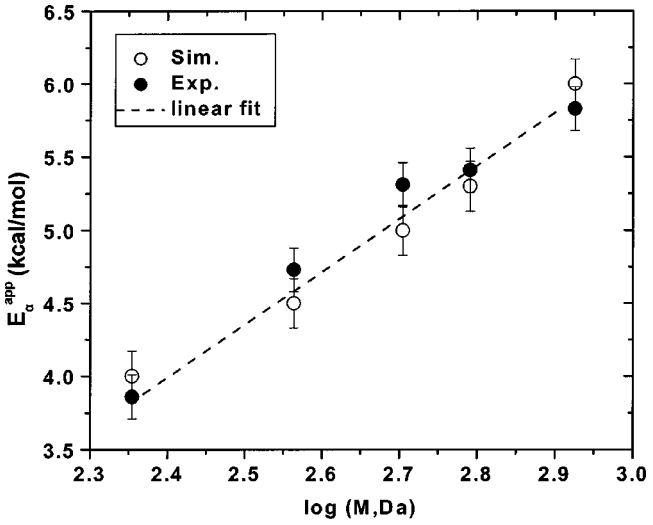

FIG. 14. Results for the apparent thermal activation energy E_a^{app} of self-diffusion of the *n*-alkane liquids as a function of their molecular weight obtained from an Arrhenius plot through the diffusivity data at various temperatures (open circles). Also shown in the figure are the experimental data of von Meerwall *et al.* (filled circles) (Ref. 13).

rises from 4.3 kcal/mol for the C_{16} alkane to 6.0 kcal/mol for the C_{60} alkane; this agrees remarkably well with the measured values. Furthermore, by using the results for the density-based excess free volume of chain ends $V_e(T)$ and the density simulation data, it is possible to fit Eq. (6) by substituting $f(T,M)$ and $\rho(T,M)$ from Eqs. (7) and (8) to the diffusivity simulation data. The fits involve two adjustable parameters: the fractional free volume $f(T,\infty)$ and the quantity $A'(=A\exp(-E_a/RT))$, both of which depend on temperature. It is found that

$$f(T,\infty)=(0.085+0.000\,65T(^\circ\mathrm{C}))\pm 0.01, \tag{15}$$

while experimentally, $f(T,\infty)=0.1+0.0007T(^\circ\mathrm{C})$. By analyzing the results for the parameter A', using an Arrhenius interpretation similar to that described above for the apparent activation energy E_a^{app}, a thermodynamic activation energy E_a for segmental jumps can be obtained averaged over all molecular weights. It is found that

$$\langle E_a\rangle_M=0.55\pm 0.30 \ \ \text{kcal/mol},$$

in reasonable agreement with the experimental value $\langle E_a\rangle_M=0.80\pm 0.25$ kcal/mol.

Figure 15(a) shows the values of D extracted from the present MD simulations with the *cis*-1,4 PI melts and how they compare to experimental data.[14] The exponent b, in particular, in the power-law dependence of D on M is found again to vary smoothly in the temperature range studied ($b=-2.6$ at 353 K while $b=-2.0$ at 413 K), as shown in Table II(b). Figure 15(b) shows the resulting $\log D$-versus-$1/T$ curves for different chain lengths. As expected, this temperature dependence can be described quite accurately by the Arrhenius relation of Eq. (14). The resulting apparent activation energies E_a^{app} are compared directly to the experimental data in Fig. 16. The very good agreement between simulations and experiments is obvious. It is confirmed that, consistently with the experimental measurements, the values of the activation energies for the *cis*-1,4 PI are greater than the corresponding values of the PE melts for the same chain length C_{60} (5.8 ± 0.3 kcal/mol for PE vs $7.\pm 1.$ kcal/mol for *cis*-1,4 PI).

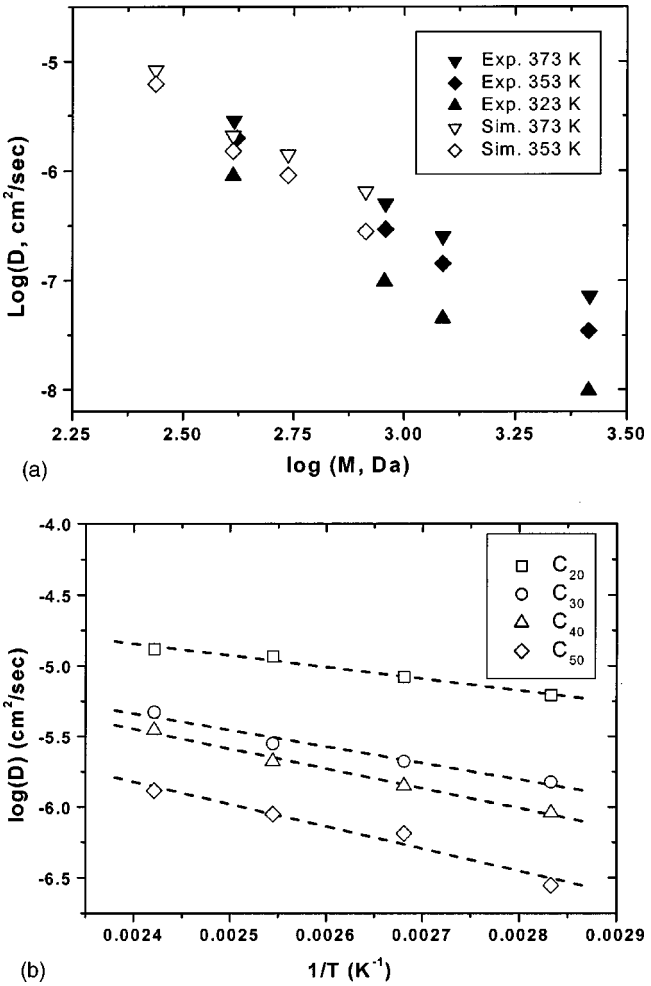

FIG. 15. (a) Self-diffusion coefficient as a function of molecular weight and comparison with experimental data for the *cis*-1,4 PI liquids. (b) Self-diffusion coefficient as a function of temperature for the *cis*-1,4 PI liquids as determined from the present *NVT* MD simulations. The temperature dependence is clearly Arrhenius, allowing us to determine an apparent activation energy (through the slopes of the dashed lines).

V. CONCLUSIONS AND FUTURE PLANS

Results have been presented from detailed atomistic simulations for the density and self-diffusion coefficient of monodisperse *n*-alkane and *cis*-1,4 PI liquids. Initially, long MC simulations were performed in the *NPT* statistical ensemble in order to equilibrate the melts and calculate their density. The relaxed configurations at the end of the MC stage were used as input to the MD algorithm in order to calculate the transport properties of these melts through equilibrium MD simulations in the *NVT* statistical ensemble. The atomistic configurations accumulated during the *NPT* MC and the *NVT* MD simulations were also analyzed geometrically; this allowed us to calculate the accessible free volume around each atom in the system, particularly around chain ends. The geometric analysis was carried out by employing the method of Greenfield–Theodorou,[19] through the construction of Delaunay tetrahedra. Linear, monodisperse *n*-alkane systems of length ranging from C_{16} to C_{60} were thus investigated at temperatures ranging from 323 to 443 K. Similar simulations were performed with *cis*-1,4 PI melts of length ranging from C_{20} to C_{60} at temperatures from 353 to 413 K.

Results about the density of both the *n*-alkane and the *cis*-1,4 PI oligomer melts were found to differ (at most) by less than 2% from the measured values. By fitting the density-versus-molecular weight M data to a hyperbolic function, we were able to estimate the contribution V_e of chain free ends to the free volume of the system, as a function of temperature T. This was compared to independent data obtained from the tessellation of space in Delaunay tetrahedra. The two sets of data were seen to be consistent with each other and with available experimental data only when the free volume around each chain end obtained directly from the geometric analysis was reduced by subtracting the corresponding free volume value around an inner atom along the chain, to define a geometrically calculated chain-end free volume, V_e^g.

The values of V_e obtained from the simulated M dependence of the density and from the geometric free-volume

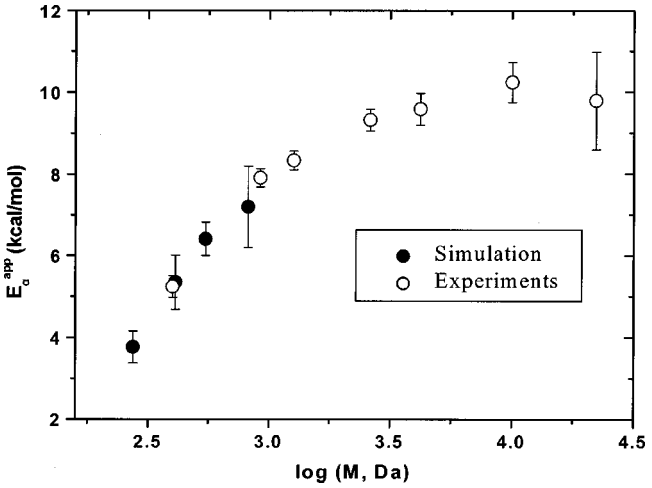

FIG. 16. Apparent activation energies for self-diffusion in the *cis*-1,4 PI systems from simulation (filled circles) as determined by the linear fit of data in Fig. 15(b). The open circles represent experimental values from Ref. 14. Both sets of data suggest greater activation energy for the *cis*-1,4 PI melts than for the *n*-alkane melts of the same molecular weight.

analysis for the *n*-alkanes were found to be in excellent agreement with recently obtained experimental results.[13] On the other hand, simulation results for the *cis*-1,4 PI oligomers suggest similar values for V_e, in contrast to older experimental data in the literature.[14] To clarify the observed discrepancy, more detailed experimental data for *cis*-polyisoprenes are needed (e.g., the exact M dependence of the density).

By applying the Einstein relation, the self-diffusion coefficient of the *n*-alkane and *cis*-1,4 PI melts was further calculated as a function of chain length and temperature. Predicted D values were found to be in excellent agreement with the recent experimental data of von Meerwall *et al.*,[13] for all systems simulated. D was seen to obey a power law of the form $D \sim M^b$, with the exponent b varying smoothly with temperature from -2.4 at 323 K to -1.9 at 443 K for the *n*-alkanes and from -2.6 at 353 K to 2.0 at 413 K for the *cis*-1,4 PI liquids. By mapping the simulation results onto the combined Bueche–von Meerwall theory for the self-diffusion of short alkanes, expressions were obtained for the fractional free volume $f(T,\infty)$ and the apparent activation energy E_a^{app} of the polymers studied as a function of temperature and molecular weight, respectively.

The present study focused on the estimation of the self-diffusion coefficient of short polymer melts and its connection with the free volume available to chain ends or the free volume available to chain ends relative to chain inner atoms. In a previous study we have calculated the transport and dynamic properties of significantly longer alkanes, up to C_{120}, whose molecular weights, however, are below the characteristic molecular weight for the formation of entanglements. The dynamic and rheological properties of these melts were obtained by two different MD approaches and gave identical results.[34,35] Current efforts are undertaken in three directions. The first considers the study of long entangled PE melts, up to C_{250}, through very long detailed MD simulations up to 300 ns.[8] The second focuses on the calculation of the self-diffusivities of *n*-alkanes in a PE matrix through MD simulations of binary blends. Results from this work will be presented in a forthcoming manuscript.[16] Finally, in a third study, simulations of longer chain *cis*-1,4 PI melts are being performed to investigate their segmental and chain dynamics and compare them directly to experimental data obtained from state-of-the-art techniques, such as dielectric relaxation spectroscopy, dynamic light scattering, quasielastic neutron scattering, etc.

[1] P. Neogi, Diffusion in Polymers (Dekker, New York, 1996).
[2] H. Ertl, R. K. Ghai, and F. A. Dullien, AIChE J. **20**, 1 (1974).
[3] S. T. Milner and T. C. B. McLeish, Phys. Rev. Lett. **81**, 725 (1998).
[4] T. P. Lodge, Phys. Rev. Lett. **83**, 3218 (1999).
[5] E. von Meerwall and R. D. Ferguson, J. Chem. Phys. **72**, 2861 (1980).
[6] G. Fleischer and M. Appel, Macromolecules **28**, 7281 (1995).
[7] M. Tuckerman, B. J. Berne, and G. J. Martyna, J. Chem. Phys. **97**, 1990 (1992); G. J. Martyna, M. E. Tuckerman, D. J. Tobias, and M. L. Klein, Mol. Phys. **87**, 1117 (1996).
[8] V. A. Harmandaris, V. G. Mavrantzas, D. N. Theodorou, M. Kröger, J. Ramírez, H. C. Öttinger, and D. Vlassopoulos, Phys. Rev. Lett. (in preparation).
[9] F. Bueche, *Physical Properties of Polymers* (Interscience, New York, 1962).
[10] M. H. Cohen and D. Turnbull, J. Chem. Phys. **31**, 1164 (1959).
[11] P. B. Macedo and T. A. Litovitz, J. Chem. Phys. **42**, 245 (1965).
[12] J. S. Vrentas and J. L. Duda, J. Polym. Sci., Polym. Phys. Ed. **15**, 403 (1977); J. S. Vrentas, C. M. Vrentas, and J. L. Duda, Polym. J. (Tokyo) **25**, 99 (1993).
[13] E. von Meerwall, S. Beckman, J. Jang, and W. L. Mattice, J. Chem. Phys. **108**, 4299 (1998).
[14] E. von Meerwall, J. Grisby, D. Tomich, and R. van Antwerp, J. Polym. Sci., Polym. Phys. Ed. **20**, 1037 (1982).
[15] E. Zervopoulou, V. G. Mavrantzas, and D. N. Theodorou, J. Chem. Phys. **115**, 2860 (2001).
[16] V. A. Harmandaris, D. Angelopoulou, V. G. Mavrantzas, and D. N. Theodorou (in preparation).
[17] M. L. Greenfield and D. N. Theodorou, Macromolecules **31**, 7068 (1998); N. Ch. Karayiannis, V. G. Mavrantzas, and D. N. Theodorou, Chem. Eng. Sci. **56**, 2789 (2001).
[18] M. Doxastakis, V. G. Mavrantzas, and D. N. Theodorou, J. Chem. Phys. (in press).
[19] M. L. Greenfield and D. N. Theodorou, Macromolecules **26**, 5461 (1993).
[20] M. Mondello, G. S. Grest, E. B. Webb III, and P. Peczak, J. Chem. Phys. **109**, 798 (1998).
[21] L. R. Dodd and D. N. Theodorou, Adv. Polym. Sci. **116**, 249 (1994).
[22] J. P. Ryckaert, G. Ciccotti, and H. J. C. Berendsen, J. Comput. Phys. **101**, 327 (1977).
[23] H. C. Andersen, J. Comput. Phys. **52**, 24 (1983).
[24] S. T. Cui, P. T. Cummings, and H. D. Cochran, J. Chem. Phys. **104**, 255 (1996); J. D. Moore, S. T. Cui, H. D. Cochran, and P. T. Cummings, J. Non-Newtonian Fluid Mech. **93**, 83 (2000).
[25] L. I. Kioupis and E. J. Maginn, Chem. Eng. J. **3451**, 1 (1998).
[26] S. Nosé, Mol. Phys. **52**, 255 (1984).
[27] W. G. Hoover, Phys. Rev. A **31**, 1695 (1985).
[28] G. D. Smith and W. Paul, J. Phys. Chem. A **102**, 1200 (1998).
[29] G. D. Smith, W. Paul, M. Monkenbush, L. Willner, D. Richter, X. H. Qiu, and M. D. Ediger, Macromolecules **32**, 8857 (1999).
[30] F. Müller-Plathe, Comput. Phys. Commun. **78**, 77 (1994).
[31] D. N. Theodorou and U. W. Suter, Macromolecules **18**, 1847 (1985).
[32] V. G. Mavrantzas, T. D. Boone, E. Zervopoulou, and D. N. Theodorou, Macromolecules **32**, 5072 (1999).
[33] N. Nemoto, M. Moriwaki, H. Odani, and M. Kurata, Macromolecules **4**, 215 (1971).
[34] V. A. Harmandaris, V. G. Mavrantzas, and D. N. Theodorou, Macromolecules **31**, 7934 (1998).
[35] V. A. Harmandaris, V. G. Mavrantzas, and D. N. Theodorou, Macromolecules **33**, 8062 (2000).